UCRL-JC-135355

The National Ignition Facility—Applications for Inertial Fusion Energy and High Energy Density Science

By
E. Michael Campbell
and
William J. Hogan

26th European Physical Society Conference on Controlled Fusion and Plasma Physics, Maastricht, Netherlands, June 14-18, 1999

August 12, 1999

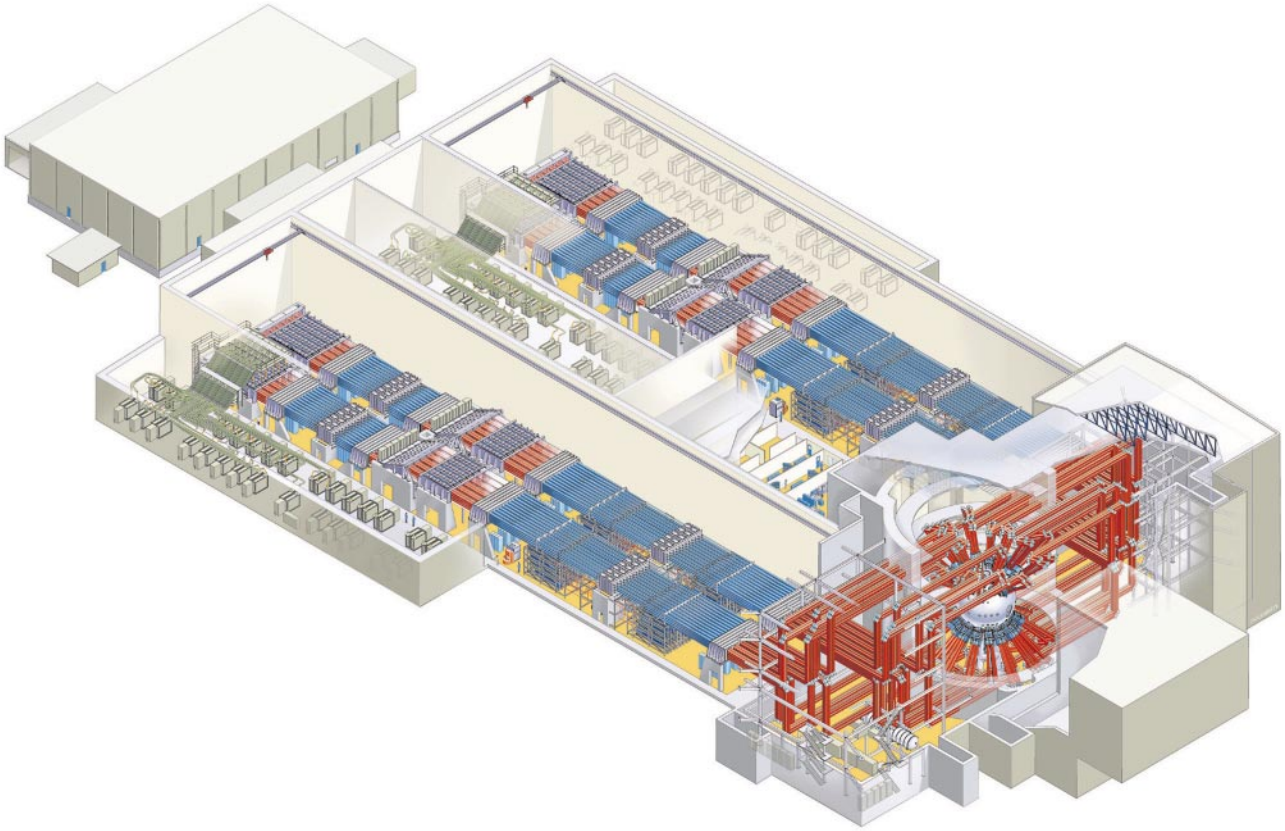

LAWRENCE LIVERMORE NATIONAL LABORATORY
University of California • Livermore, California • 94550

The National Ignition Facility—Applications for Inertial Fusion Energy and High Energy Density Science

E. Michael Campbell
William J. Hogan

I. Introduction

Over the past several decades, significant and steady progress has been made in the development of fusion energy and its associated technology and in the understanding of the physics of high-temperature plasmas. While the demonstration of net fusion energy (fusion energy production exceeding that re- quired to heat and confine the plasma) remains a task for the next millennia and while challenges remain, this progress has significantly increased confidence that the ultimate goal of societally acceptable (e.g. cost, safety, environmental considerations including waste disposal) central power production can be achieved.

This progress has been shared by the two principal approaches to controlled thermonuclear fusion—magnetic confinement (MFE) and inertial confinement (ICF). ICF, the focus of this article, is complemen- tary and symbiotic to MFE. As shown in Figure 1, ICF invokes spherical implosion of the fuel to achieve high density, pressures, and temperatures, inertially confining the plasma for times sufficiently long ($t \sim 10^{-10}$ sec) that ~30% of the fuel undergoes thermonuclear fusion.

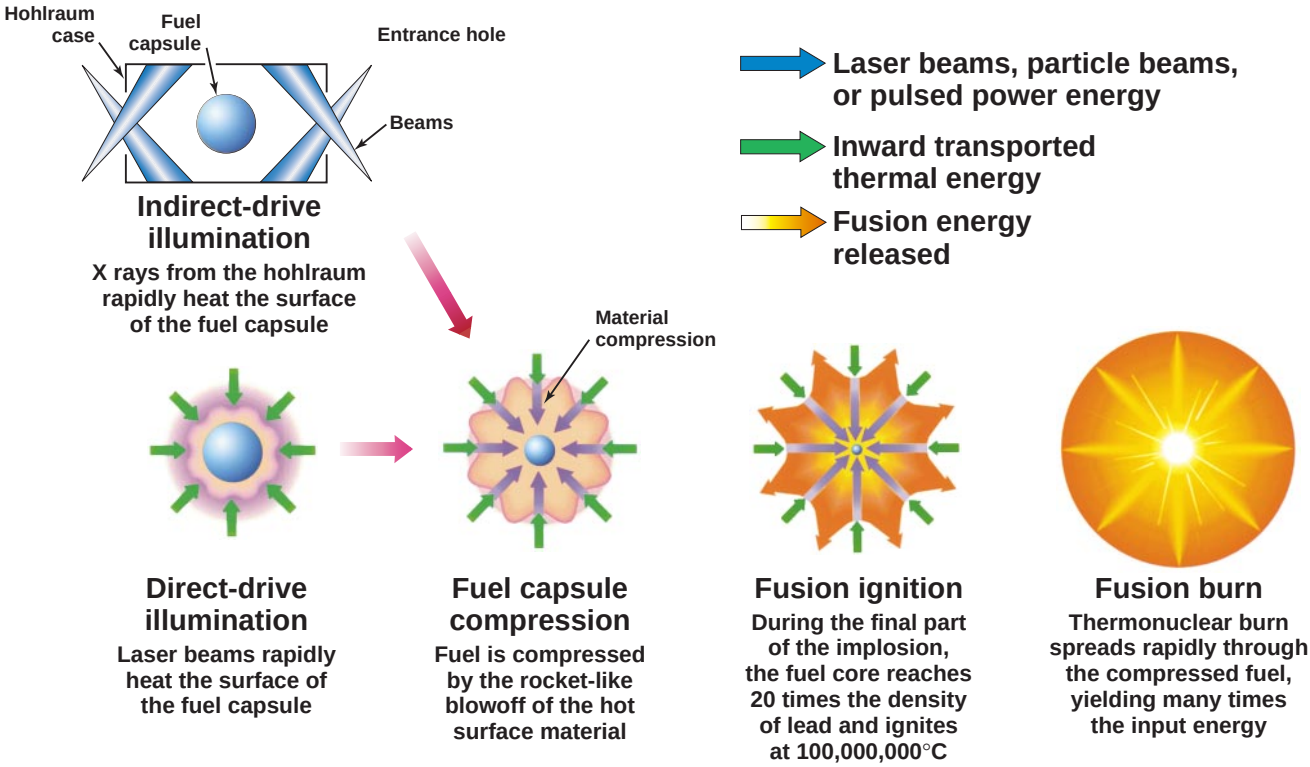

Figure 1. Four steps of the inertial confinement fusion (ICF) process.

The unequivocal demonstration of the physics of ICF including fusion energy gain is planned for the National Ignition Facility (NIF) and Laser Megajoule (LMJ) now under construction in the United States and France respectively within a decade.

In addition to fusion research, lasers and pulsed power facilities developed for ICF have proven to be outstanding research tools for the study of high energy density science. Lasers and pulsed power reproducibly concentrate energy in space and time and thus can create diagnosable plasmas that exist for picoseconds to tenths of microseconds at extremely high energy density. Such experiments can reach plasma electron and ion temperatures greater than 10^8 K, pressures greater than 10^{11} atmospheres, and radiation temperatures greater than 3.5×10^6 K. For example, using cylindrical gold hohlraums with diameters of 1, 1.6, and 4.8 mm on the Nova laser, radiation temperatures of 288 eV, 151 eV, and 94 eV have been created for times from 1 to 15 nsec.[1] The resulting radiation fluxes of greater than 10^5 GW/sr/cm^2 can be used for fusion capsule compression or for a variety of measurements of basic material properties and/or physical processes. Large laser facilities doing such experiments include Nova, Omega, and Nike in the United States, Gekko XII in Japan, Phebus in France, Helen and Vulcan in the United Kingdom, and Iskra in Russia. Many other countries have smaller facilities but nevertheless are able to do outstanding science on them because even small lasers can achieve extreme repeat- able and diagnosable conditions.

Furthermore, recent advances in sub-picosecond laser technology have opened new opportunities for the production of matter at ultra high specific energies ($\varepsilon > 10^{10}$ joules/gram). Such high brightness lasers can now routinely achieve irradiances $>10^{20}$ W/cm^2 and make possible, for example, the study of relativistic plasmas.[2]

In this article we will briefly describe the features and development plan for inertial fusion (Section II) and the National Ignition Facility and its role in fusion energy development (Section III). Section IV will highlight some of the science in the fields of astrophysics, shock and condensed matter, and nuclear physics that are derived from ICF research. Section V will provide a short summary and hopefully communicate the excite- ment and challenge for the field over the next decade.

II. Inertial Fusion and IFE Development Plan

As shown in Figure 1 and briefly described above, ICF relies on the inertia of the fuel mass to provide confinement sufficiently long that a significant fraction of the fuel (~20–30%) undergoes thermonuclear fusion. A spherical fusion capsule consists of an outer region, the ablator (consisting of doped plastic, polyamide, or beryllium), and an inner cryogenic shell of frozen equimolar deuterium-tritium. A driver (laser, ion beams, pulsed power), which can concentrate energy in space and time, generates a flux exceeding 10^{15} W/cm^2 which rapidly heats and vaporizes the ablator. The ablator rapidly expands out- ward and imparts radial inward momentum to the remaining shell. This spherical, ablation-driven rocket reaches implosion velocities in excess of 3×10^7 cm/sec. The energy that can be delivered to the fuel is the product of the ablation pressure (a product of the areal mass ablation rate and exhaust velocity), typically 100 Mbar, and the volume enclosed by the shell (ignoring the volume of the final compressed state).

Implosion amplifies the ablation pressure a thousandfold and in its final configuration, the fuel is nearly isobaric at pressures up to ~200 Gbar but consists of two effectively distinct regions—a central hot spot containing ~2 to 10% of the fuel and a dense, but cold Fermi degenerate main fuel region comprising the remaining mass. Fusion initiates in this central region where the hydrodynamic work and alpha particle deposition exceed conduction and radiation losses, and a thermonuclear burn front propagates radially outward into the main fuel, producing high gain ($G > 50$). The efficient assembly of the fuel into this configuration places stringent requirements on the details of the driver coupling, including the time history of the irradiance and the hydrodynamics of the implosion.

Figure 1 also shows the two principal approaches to ICF: indirect drive, where the driver energy is first converted into x rays in a high atomic number hohlraum that encloses the capsule with a characteris- tic Planckian temperature of 250–300 eV; direct drive, where the capsule is directly illuminated by the driver. Significant progress has been made in these two approaches, and today they both appear viable for achieving high gain.

With such targets producing high gain, an IFE power plant as shown in Figure 2 will consist of four components: (1) a driver which must efficiently ($\eta > 5\%$) and economically (cost <$1B) produce the concentrated power (>500 TW) and energy (>~2 MJ) to drive a fusion implosion 5 times or more a second ($<P>_{Driver} > 10$ MW); (2) a target factory that economically (~$0.3/target) produces ~$3 \times 10^8$ high gain targets a year; (3) a target chamber that enables the successful injection of the IFE targets and the propaga- tion of the driver energy, contains the fusion explosion ($E_{fusion} > 200$ MJ) and breeds tritium—all in an environmentally acceptable and cost-effective manner, and (4) a balance of plant that must efficiently (>40–50%) convert the high-grade fusion energy into electricity for the power grid.[3]

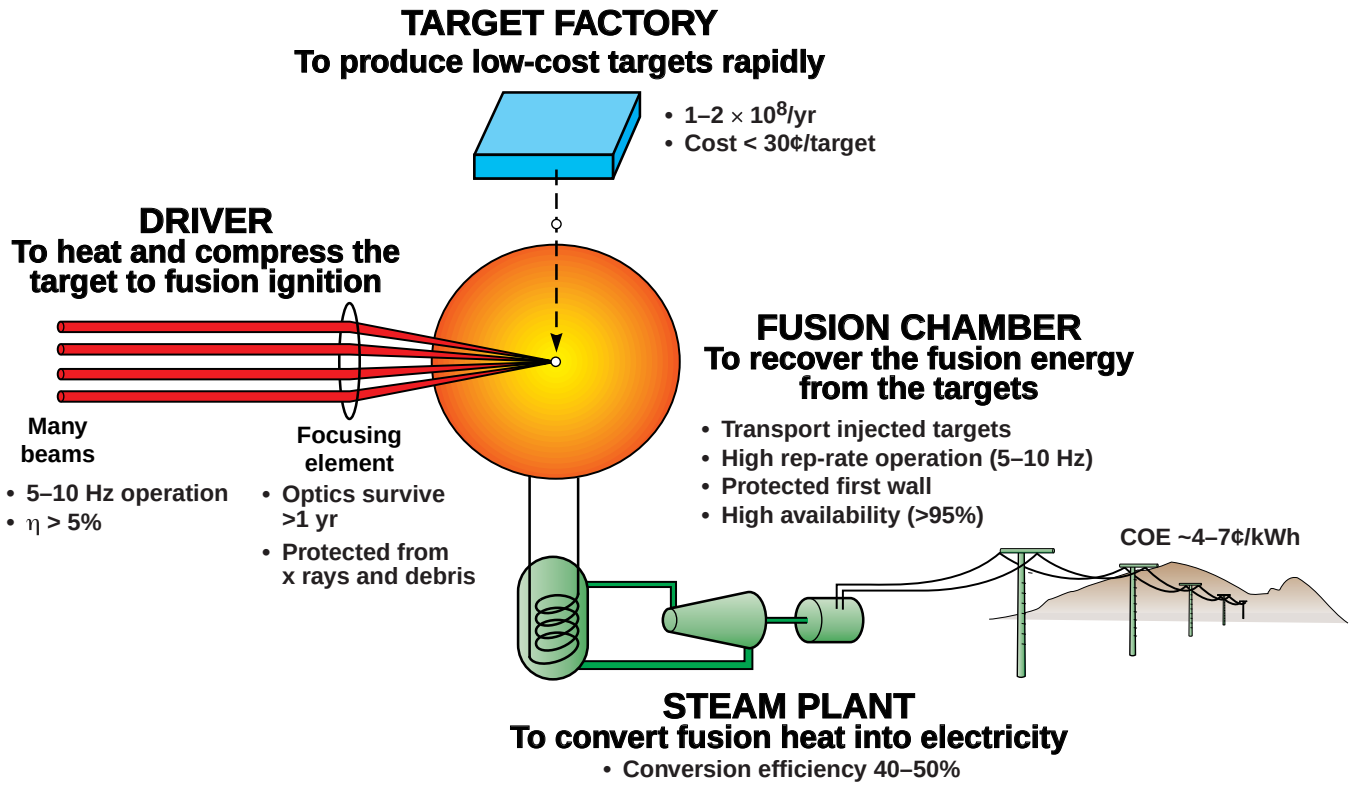

Figure 2. Inertial fusion energy (IFE) power plants will consist of four parts.

To produce affordable electricity from IFE (Cost of elctricity [COE] in the range of 4–7¢/kW-hr) that is environmentally acceptable (plant components that allow for shallow burial and no off-site evacuation in a worst case accident) presents many challenges. Target energy gains of 30 to more than 100 (depending on the driver efficiency) are required to keep the recirculating power low[3,4] From Figures 1 and 2, IFE also has many attractive features that include: (1) separability of the plant components allowing for parallel development and "local" optimization; (2) a high degree of modularity in components (for example, the driver would consist of hundreds to thousands of identical beamlines) allowing for cost- effective development, full-scale engineering and scientific prototypes, and economy of scale in manufac- turing; (3) multiple, credible options in targets (direct and indirect), drivers (lasers, ions, possibly pulsed power), and chambers (ranging from neutronically thick liquids or dry walls facing the fusion explosion).

Another extremely important feature for IFE development is that, as will be discussed in the next section, it leverages the extensive target physics program supported by DOE for national security pur- poses, the accelerator development supported by the high energy physics community , and industry for the development of lasers.

Given the progress in the field and the attractive features of IFE, a development plan has been formulated by the community that, if funded and successful, would lay the technical foundation for beginning construction of an engineering test facility (ETF) in the second decade of the next century . The goal of this facility would be to produce average fusion power (in the range of 100 to 400 MW) and demonstrate the operability, environmental and safety features, and the economics of IFE for a project cost in the range of $2B to $3B.

The development program has been formulated with the entire fusion community into a "road map" that is shown in Figure 3. This IFE specific version shows the different stages of development and demonstration: concept exploration, proof of principle, performance extension, and fusion energy development (the ETF) leading to a demonstration plant. To progress to higher, more costly stages, specific scientific and technical objectives must be met. The existing ICF program engages the road map at the first three levels with significant ongoing investment by DOE's national security program (illus- trated by the shaded region in the performance extension). Examples of activities in the first level include exploring ways of extending the successful Z pinch efforts into an IFE concept (rep-rate, stand-off, waste stream), examination of the high gain (G > 200) "fast ignitor" concept where isochroically compressed fuel is ignited by a separate high-intensity driver, and the exploration of high-

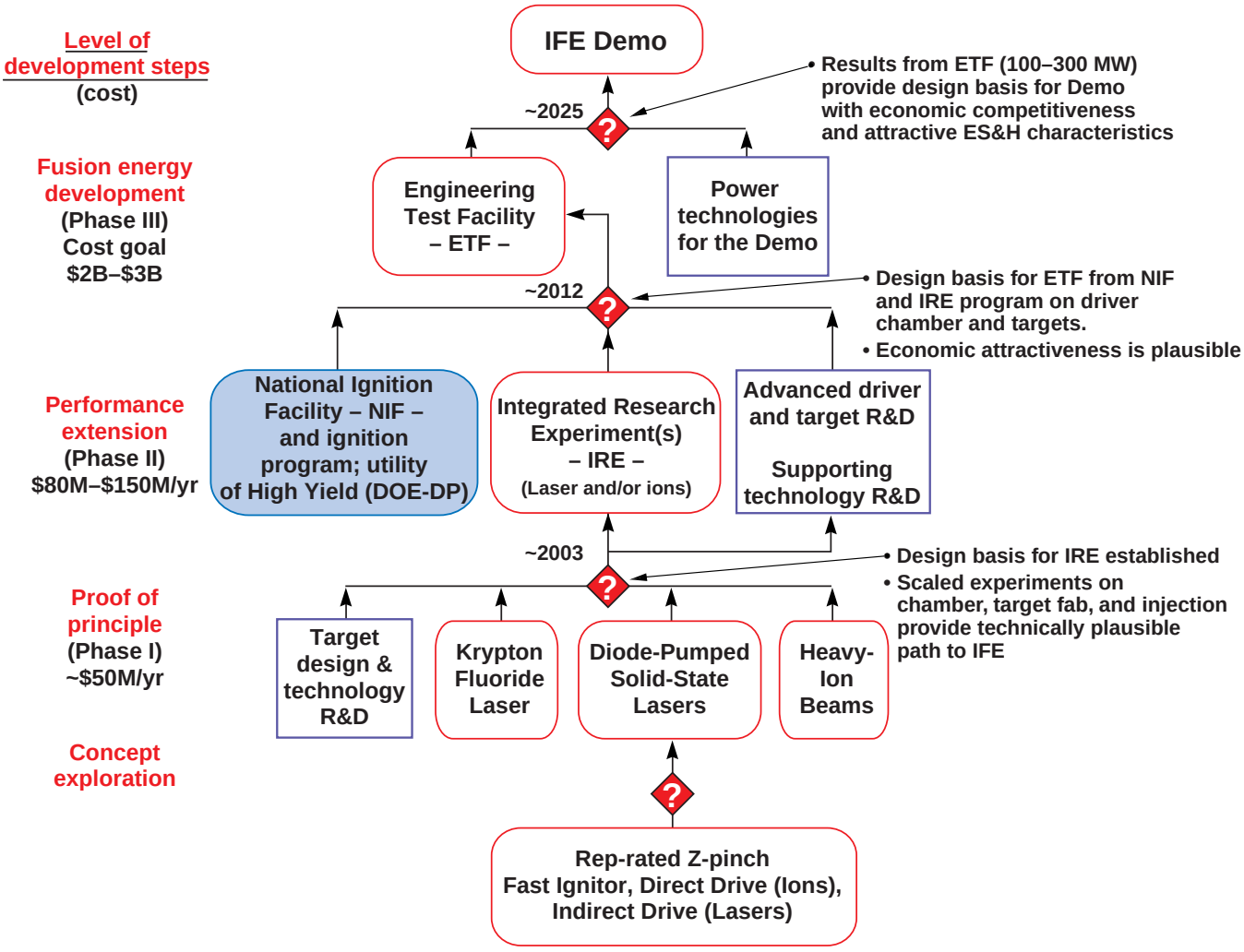

Figure 3. The Inertial Fusion Development Strategy is integrated with the Fusion Energy Road Map.

gain (G > 100) indirect drive with lasers. Examples of the second stage include the development of high rep rate (>5 Hz) 100 joule- class KrF (the Electra project at the Naval Research Laboratory) and diode-pumped solid-state lasers (Mercury project at LLNL). Mercury and its goals are shown in Figure 4.

The third level includes the demonstration of ignition and gain on the single-shot National Ignition Facility (NIF) and the construction of high rep rate, multikilojoule (~15 kJ to 300 kJ) drivers that also address key chamber issues (driver chamber interface, beam propagation in the chamber, etc.). Because of these system objectives, these facilities have been named integrated research experiments (IRE), and a heavy-ion example, along with its objectives, is displayed in Figure 5.

The results of the IREs and the target physics from NIF, described in the next section, would form the basis of proceeding with an Engineering Test Facility .

III. The National Ignition Facility (NIF)

Demonstration of the critical features of IFE targets, that is ignition and propagating thermonuclear burn, is a principal goal of the NIF, now under construction at Lawrence Livermore National Laboratory (LLNL).5 A schematic of the 192-beam, flashlamp-pumped, Nd: glass laser facility, whose output is frequency up-converted to an on-target wavelength of 0.35 mm is shown in Figure 6. The nominal output specifications of NIF are shown in Table 1, and the state of construction as of June 1999, including the 10- meter-diameter target chamber, is shown in Figure 7. NIF is scheduled for completion in late 2003, with ignition and gain experiments beginning in 2006–2007. As shown in Figure 8, NIF is an extremely flexible facility with the ability to irradiate both indirect- and direct-drive targets with a variety of pulse formats including the complicated pulses required for high-gain ICF.

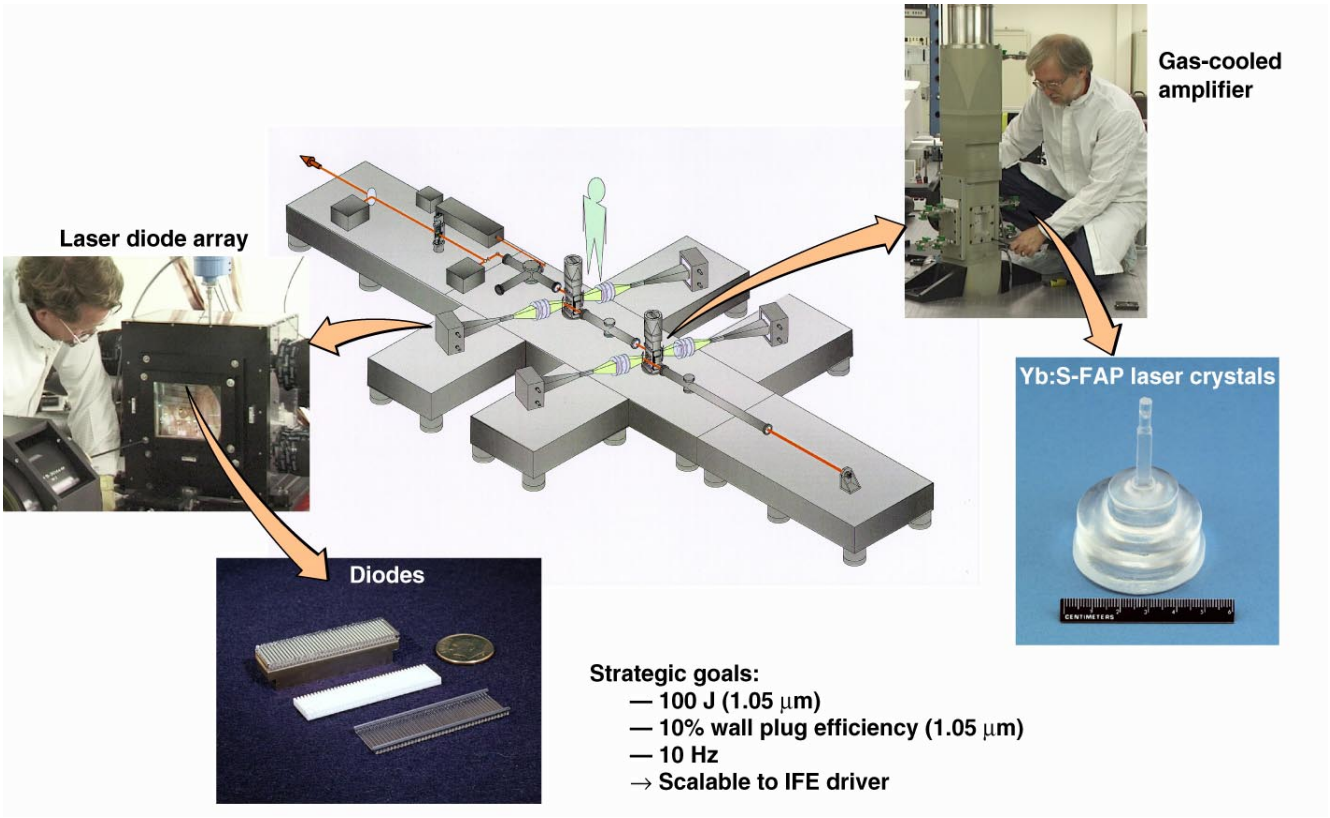

Figure 4. The Mercury laser: An example of an IFE-related laser activity over the next several years.

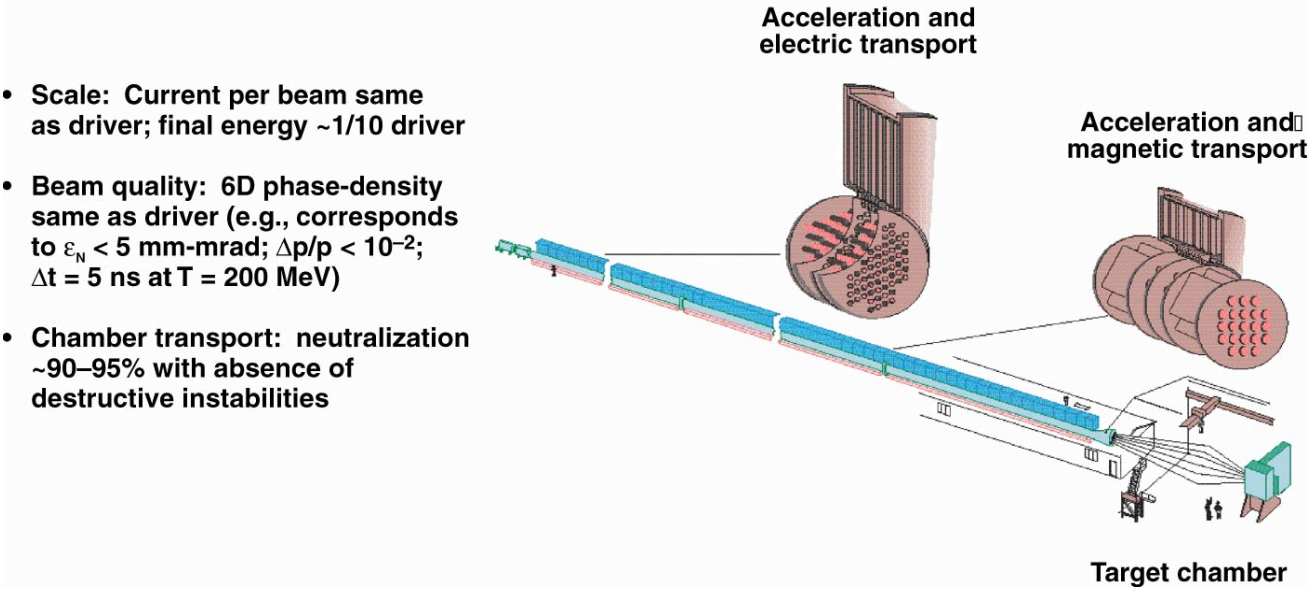

Figure 5. Heavy-ion Integrated Research Experiments (IREs) will play a major role demonstrating the feasibility of IFE: example, heavy ions.

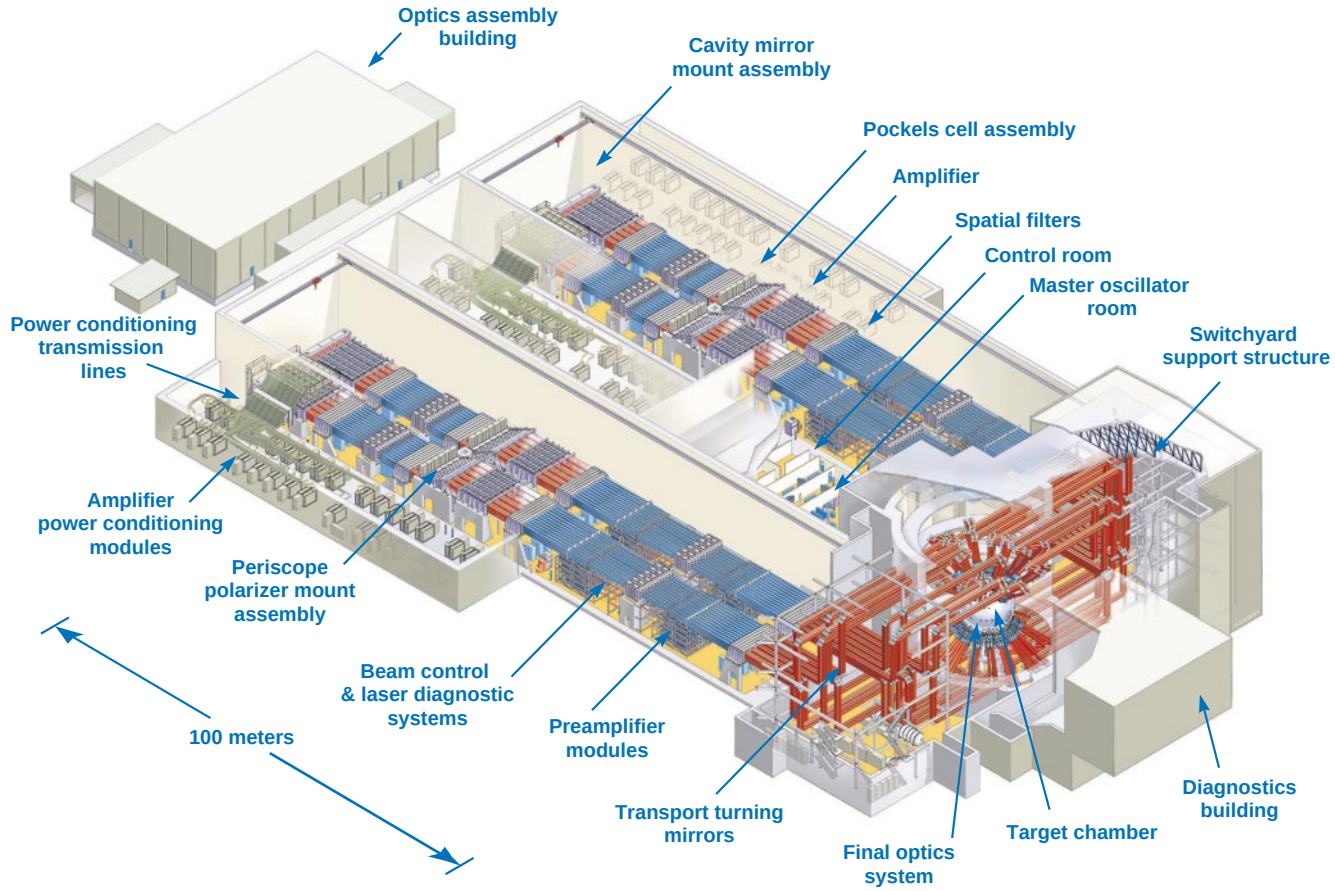

Figure 6. The National Ignition Facility and the LMJ will provide a unique opportunity for demonstrating critical elements of ICF target physics required for IFE.

Table 1. NIF top-level performance requirements.

Laser pulse energy (on target)	**1.8–2.5 MJ (pulse shape dependent)**
X-ray backlighting	**Beams independently timed and located**
Laser pulse shaping	**Flexible (0.1 – >20 nsec in complicated pulse shapes)**
Laser pulse peak power	**>500 TW**
Laser pulse wavelength	**0.35 μm**
Beam power balance	**<8% rms over 2 ns**
Beam pointing accuracy	**<50 μm**
ICF target compatibility	**Cryogenic and noncryogenic**
Annual fusion yield compatibility (indirect and direct drive)	**50 shots with yield 20 MJ 1200 MJ/y annual yield**
Maximum DT fusion yield/shot	**(~100 MJ)**
Experiments/year *	**>700**

* Program is now under way with UK collaboration to increase the shot rate to >1000.

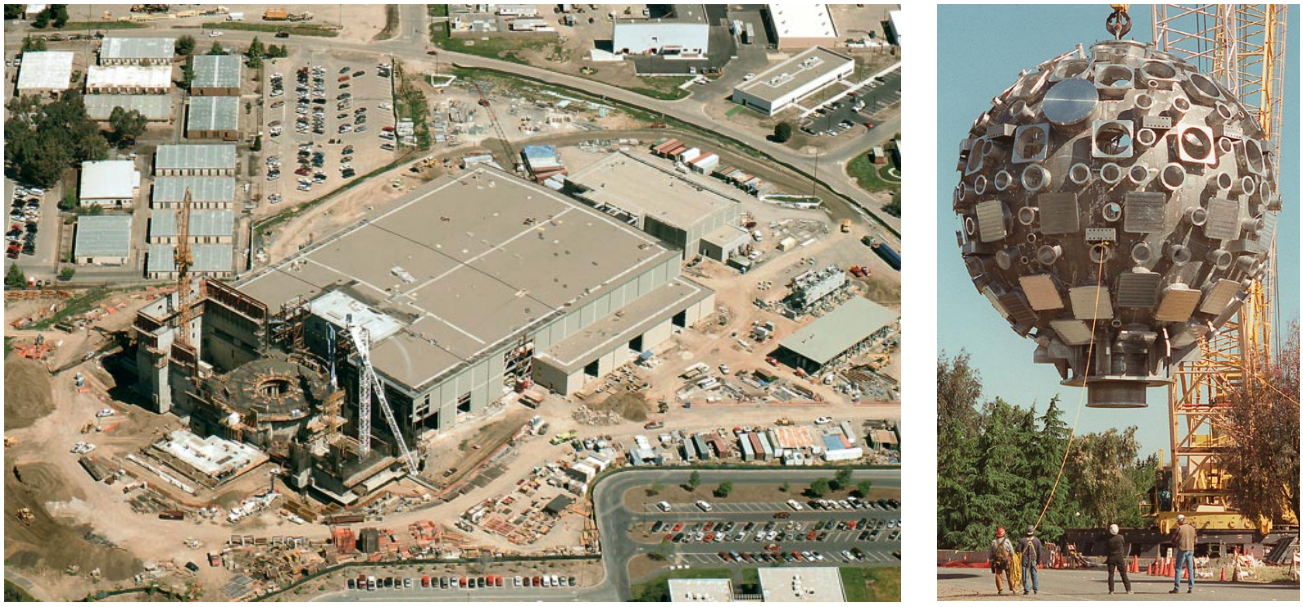

Figure 7. Aerial view of NIF looking north (April 23, 1999); moving target chamber (June 6, 1999).

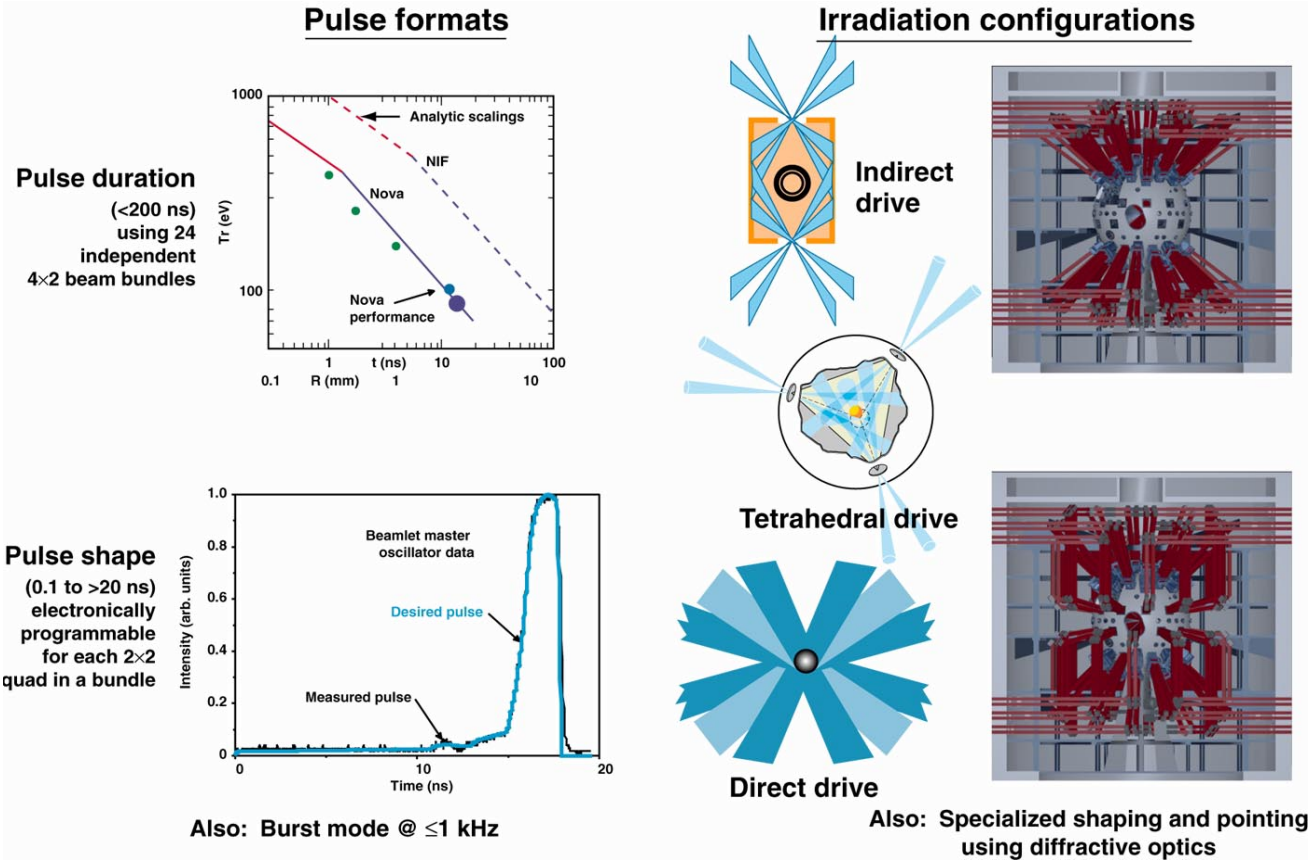

Figure 8. The NIF will be a flexible, versatile facility.

As mentioned in the previous paragraph, the principal goal of NIF is to demonstrate ignition and modest gain. Figure 9 shows the gain curves calculated over the range of operating conditions for NIF. The physics of indirect and direct drive are well established whereas the predicted impressive gains for the fast ignitor are based on models, which have not yet been validated by experiment. The baseline indirect- and direct-drive targets, which have nominal gains of 10 and 30, are shown in Figure 10 (which also illustrates the pulse format flexibility of NIF). Numerous target designs, with absorbed energies greater than 900 kilojoules, calculate to ignite and burn.

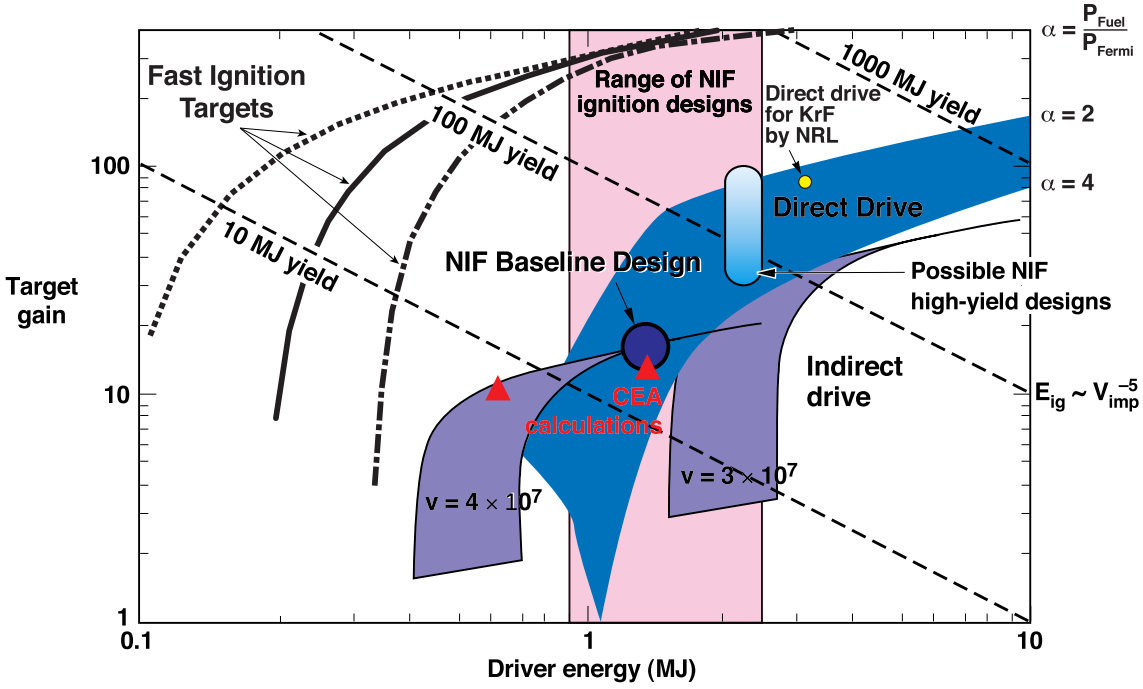

Figure 9. NIF will map out ignition and gain curves for multiple target concepts.

(a) (b)

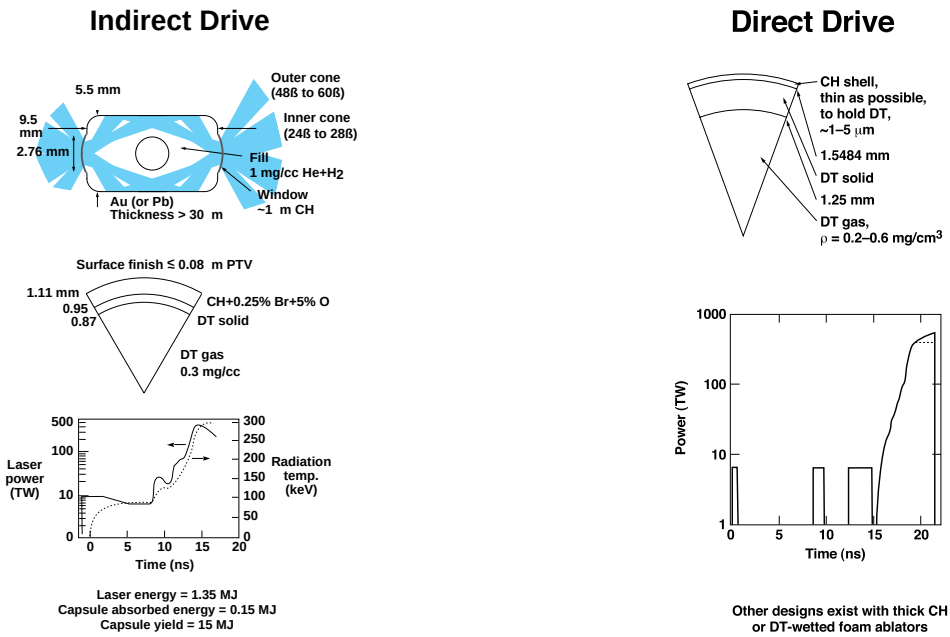

Figure 10. NIF baseline indirect (a) and direct (b) target designs along with the laser pulse shapes used to drive them.

More recently, work exploring higher gain on indirect drive has shown promise. In Figure 11, the energy-power parameter space available on NIF is shown along with the location of the nominal gain 10 design and one with gain 30. As shown in the figure, by optimizing the hohlraum and laser, it may be possible to produce indirect-drive targets where the capsule absorbs >600 kJ of x rays (the baseline NIF capsule absorbs 150 kJ of x rays). Such targets would produce gains greater than 50![6]

- **Lower power, longer pulse shapes can give more energy from NIF (260 eV vs 300 eV)**
- **Material mixtures ("cocktails") reduce hohlraum wall losses**
- **Slightly larger capsule/hohlraum size increases coupling efficiency to capsule**
- **Longer pulses increase the radiation fraction absorbed by a capsule**
- **Slight LEH closure reduces hole losses**

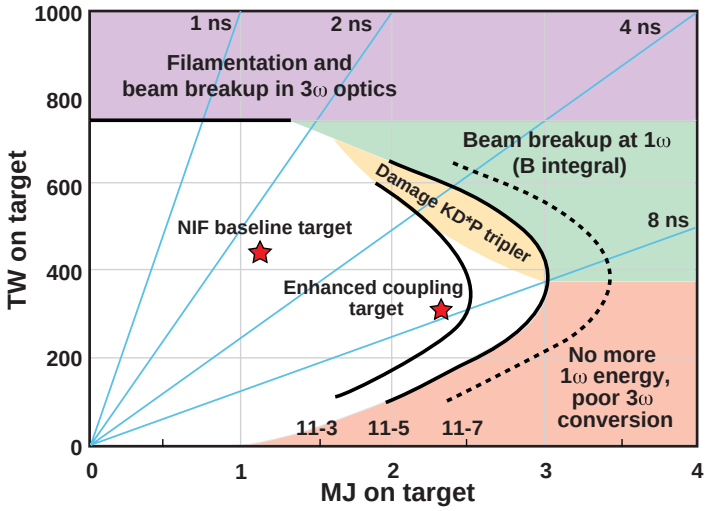

Figure 11. We are exploring ways to increase the capsule energy on NIF for indirect-drive designs.

For IFE to be successfully developed, target gains of 30 to more than 100 are required. The exact target gain depends upon the driver efficiency in converting electrical energy into beam energy. For an economical power plant, the product of driver efficiency and target gain should be larger than about 10.[3,4] For laser drivers, driver efficiencies of 7–15% may be attainable.[7] Therefore, target gains of 70 to 140 are needed. For heavy-ion drivers, efficiencies of 25 to 35% may be possible,[8] thus requiring gains of 30 to 40. NIF is expected to obtain ignition and gains of 10 (although recent work suggest that higher gains are possible). Targets igniting on NIF must be related to the targets that can obtain the necessary gain for an economical power plant.

The key to relating target ignition on NIF to the requirements for high gain is to look in detail at target ignition and propagating burn. A single parameter like target gain is insufficient to understand this relationship. Figures 12a and 12b show the ignition and propagating burn processes to be demonstrated on NIF. Figure 12a shows the configuration of a compressed, heated high-gain target at the time of ignition. At peak compression, the isobaric fuel is composed of a hot (10 keV), low-density hot spot and a dense ($\rho > 400$ g/cm^3), low-temperature, near-Fermi degenerate main fuel. If the hot-spot areal density (ρr) exceeds 0.3 g/cm^2 (an alpha range), the alpha particles will deposit their energy locally and boot- strap the temperature achieved through the PdV work of the compression. As the hot-spot temperature bootstraps upward, the reaction rate increases. Alpha particles produced near the edge of the hot spot will deposit their energy into the surrounding layer of cold compressed fuel to start a propagating thermonuclear burn front. This burn wave will propagate through the cold surrounding fuel, which must have a ρr of 2–3 g/cm^2. At this value, 1/4 to 1/3 of the fuel will be burned. NIF must not only demon- strate ignition but must also demonstrate self-sustained propagating burn so that if a greater mass of fuel is compressed, there will be confidence that the propagating burn front will consume the additional fuel.

Figure 12b shows the temperature-ρr map of possible conditions in an ICF target. Ignition and propagating burn are only possible in a target when the gains due to PdV work and alpha particle deposition are greater than the losses due to heat conduction and radiation. In this map we have shown the dividing line between the regions where gains or losses dominate for an implosion velocity of 3×10^7 cm/s. This map shows the region achievable on Nova and that achievable on NIF. NIF target implosions must move through this map staying in the gain region. This is sometimes referred to as moving through the "hole" in the Wheeler diagram (after John Wheeler of Princeton University who first suggested this as a criterion for inertial fusion ignition).

(a) (b)

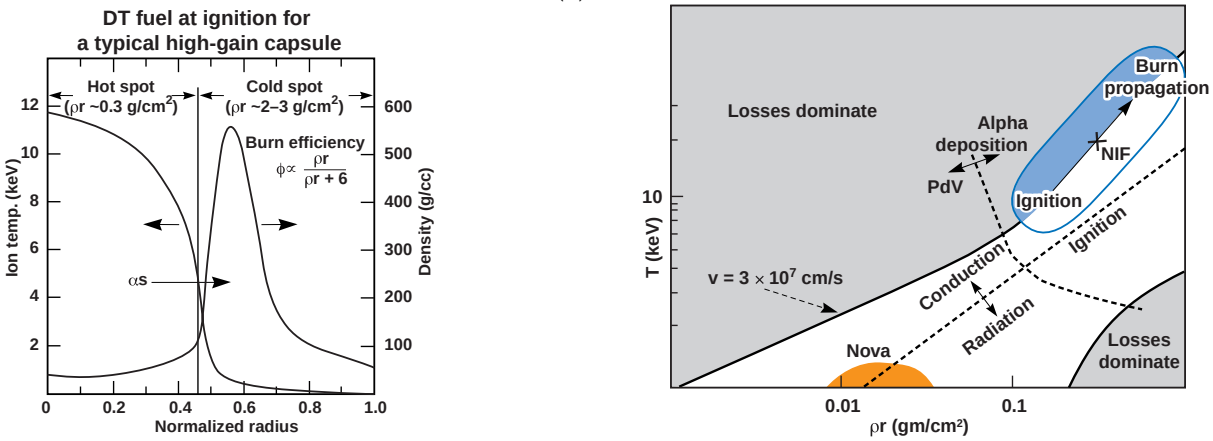

Figure 12. The increased energy of NIF allows a large enough fuel-areal density for fusion ignition and propagating burn.

Nova experiments have achieved a ρr of about 0.02 g/cm^2, a temperature of about 1 keV and a gain of 0.001.[9] With NIF we expect a ρr of ~1 g/cm^2, temperatures of about 10 keV (with alpha particle deposition augmentation) and, therefore, expect a gain of order 10.[10]

Detailed simulations of both NIF ignition targets and high-gain targets have been used to design the ignition target to be "hydrodynamically" equivalent to the high-gain target. By that we mean that up to the point that the ignition target runs out of compressed cold fuel, the physics of ignition and propagating burn in the NIF ignition target mimics what would go on in a high-gain target. The propagation issues for high- gain capsules will be settled by ignition and propagating burn experiments on NIF.

Figure 13a shows the details of the calculated temperature and density profiles for both ignition (0.2-MJ capsule absorbed energy) and high-gain (2-MJ capsule absorbed energy) targets. Figure 13b shows the ion temperature vs ρr profile at various times during the burn of each capsule. The ignition target is shown as the set of solid lines while the high gain target is shown as the set of dashed lines. The ignition capsule quenches due to disassembly at a ρr of 1–1.5 g/cm^2. However, up to that point, its profile is very similar to that of the high-gain target. Therefore, we would expect that the demonstration of ignition and modest gain in the ignition target would be sufficient to have high confidence that high gain could be achieved with a driver large enough to compress an increased fuel mass. In addition to this type of analysis, DOE is also exploring the value of a single-pulse high-yield fusion explosion which would result from a higher mass implosion. This study may identify a need for a high-yield post-NIF facility for national security purposes.

(a) (b)

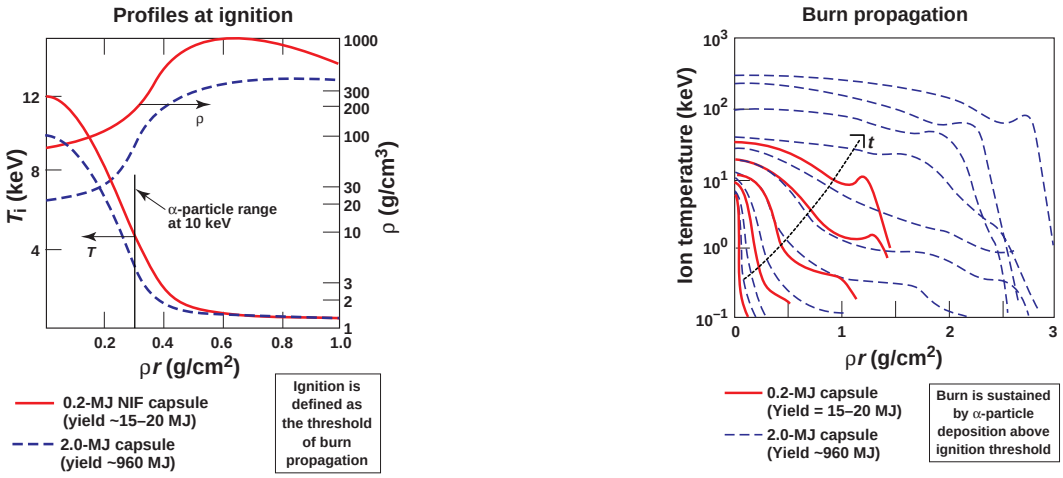

Figure 13. (a) Temperature and density profiles for both ignition (0.2-MJ capsule absorbed energy) and high-gain (2-MJ capsule absorbed energy) targets to a ρr of 1 g/cm^2. (b) Ion temperature vs ρr at a variety of times in capsule burn for the ignition and high-gain targets.[11]

IV. High Energy Science from ICF

For the past several years a modeling and experimental program has been under way to explore the utility of ICF science and facilities in the areas of astrophysics, planetary science, and shock and con-densed matter physics. Experiments are now under way in the areas of supernovae explosion hydrody- namics, radiative jets (Herbig-Haro objects), solid-state flow relevant to the interiors of terrestrial planets, photoablation, ablation front instabilities (the "pillars of creation" recorded by the Hubble telescope), and equation of state along the principal Hugoniot of hydrogen (relevant to the Jovian planets and Brown dwarfs) and other materials. This work has been very successful and several illustrative examples are shown in this section.

Supernova Explosion Hydrodynamics

Figure l4 shows the striking similarity of the hydrodynamic instabilities between an imploding ICF capsule and an exploding core collapse supernova. It can be shown that such physics are well described by Euler's equation

$$\frac{\delta \bar{V}}{\delta t} + (\bar{V} \cdot \nabla)\,\bar{V} = \frac{-\nabla P}{\rho}$$

and by making the following scale transformations

$$\rho = A_1\,\rho$$
$$P = A_2\,P$$
$$\bar{X} = A_3\,\bar{X}$$
$$\tau = \left(\frac{A_1}{A_2}\right)^{1/2} A_3$$

The physics are Eulerian invariant. Figure 15 shows that, by proper design of a laboratory experiment, the calculated velocity, density, and pressure profiles of a supernova explosion can also be reproduced. With this motivation, recent planar experiments have validated hydro instability codes utilized in supernova calculations.

Figure 16 shows the experimental arrangement, x-ray radiograph, and model/data comparisons of Richtmyer-Meshkov and Rayleigh-Taylor instability growth at the Cu-CH interface of an accelerated target employed in the laboratory experiments. Excellent agreement is observed. Recent striking experiments, shown in Figure 17, display the explosive phase of an x-ray heated cylinder, which qualitatively compares quite well to the calculated supernova explosion.

Simulations of possible experiments on NIF have been done to explore the expanded capabilities NIF will bring. Figure l8 shows the highly nonlinear turbulent mixing that is calculated to occur in such experiments and compares it with simulation of supernova 1987A. Based on these types of calculations and the experiments that have been conducted on Nova and elsewhere, NIF should make a major contribution to our understanding of the nonlinear hydrodynamics of supernovae explosions.

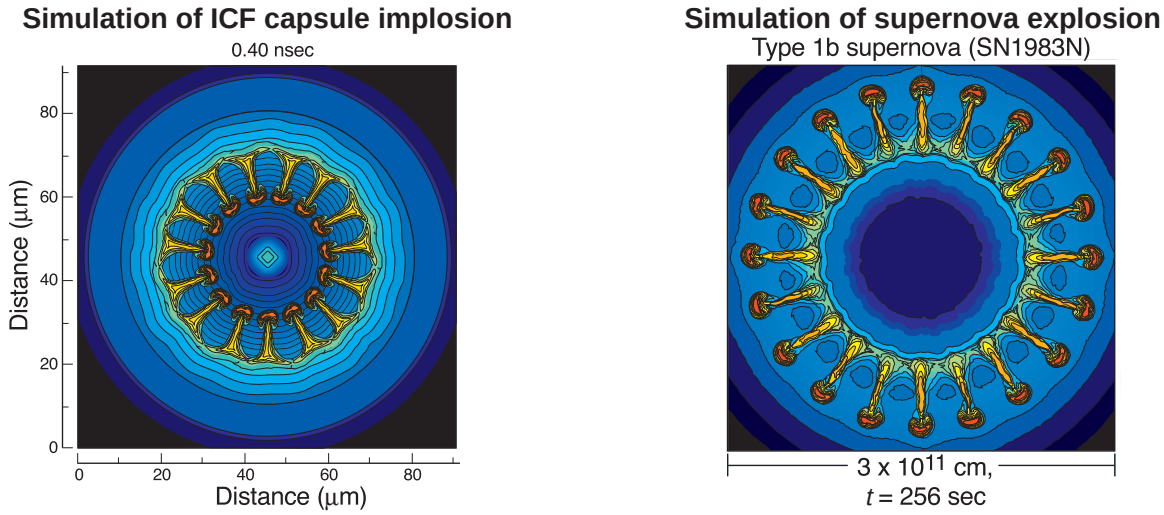

Figure 14. Striking similarities exist between hydrodynamic instabilities in ICF capsule implosions and core-collapse supernova explosions.[12, 13]

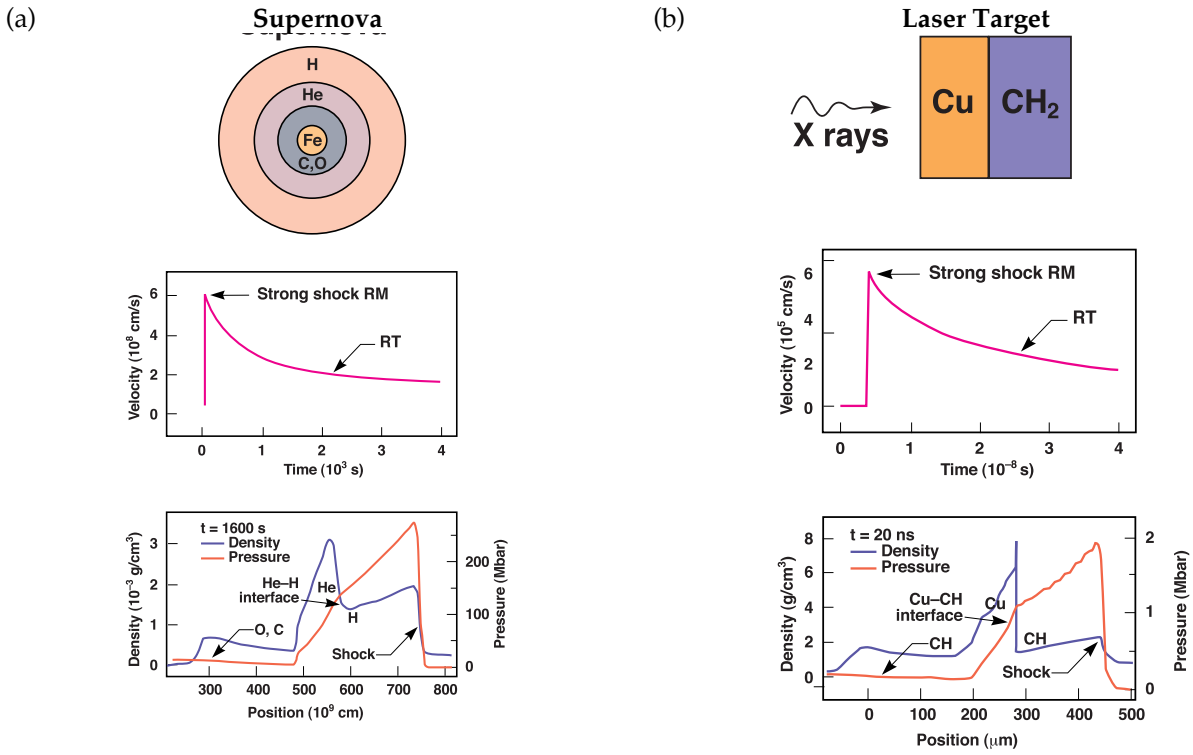

Figure 15. **Velocity, density, and pressure profiles for a supernova (a) that are reproduced in a laboratory experiment driven by laser-generated x rays (b).[14]**

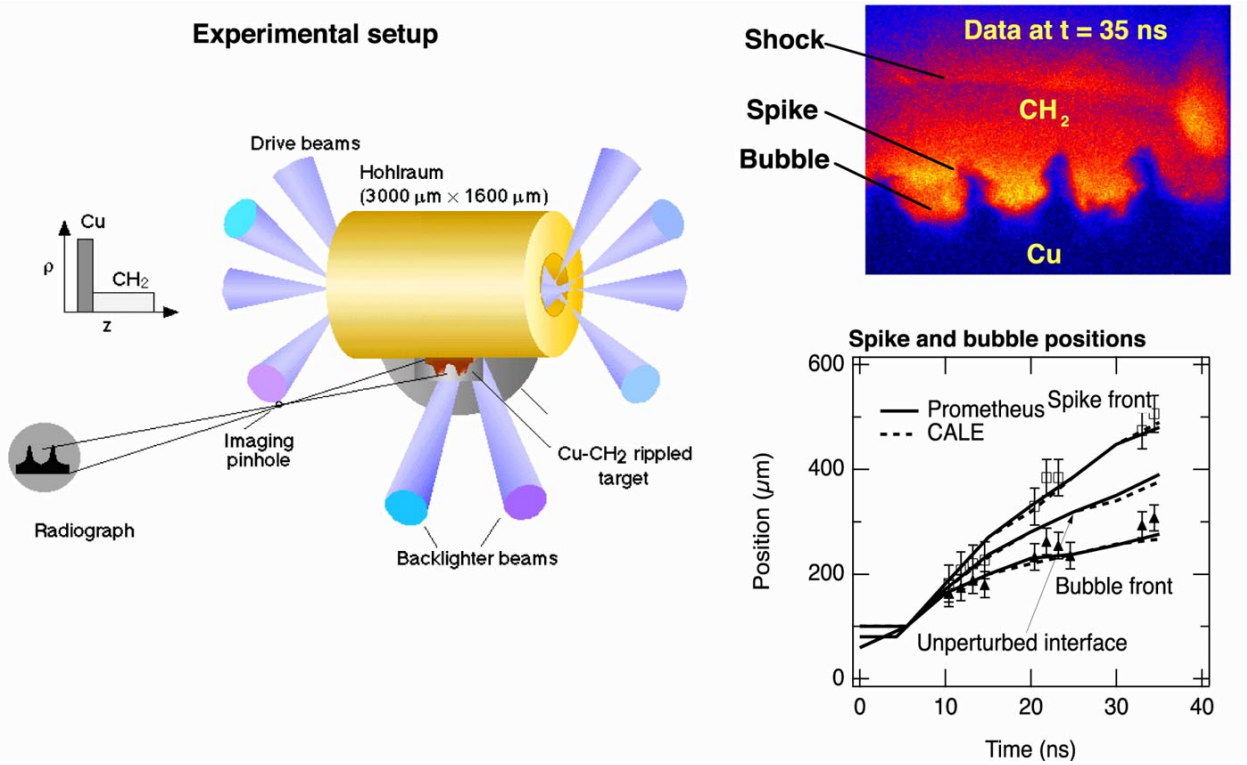

Figure 16. **Scaled core-collapse supernova experiments on the Nova laser mimic the hydrodynamics at the helium-hydrogen interface with surrogate materials. Bubbles, spikes, mushroom caps are observed, and bubble and spike positions are simulated with supernova code PROMETHEUS, and with CALE.[15, 16]**

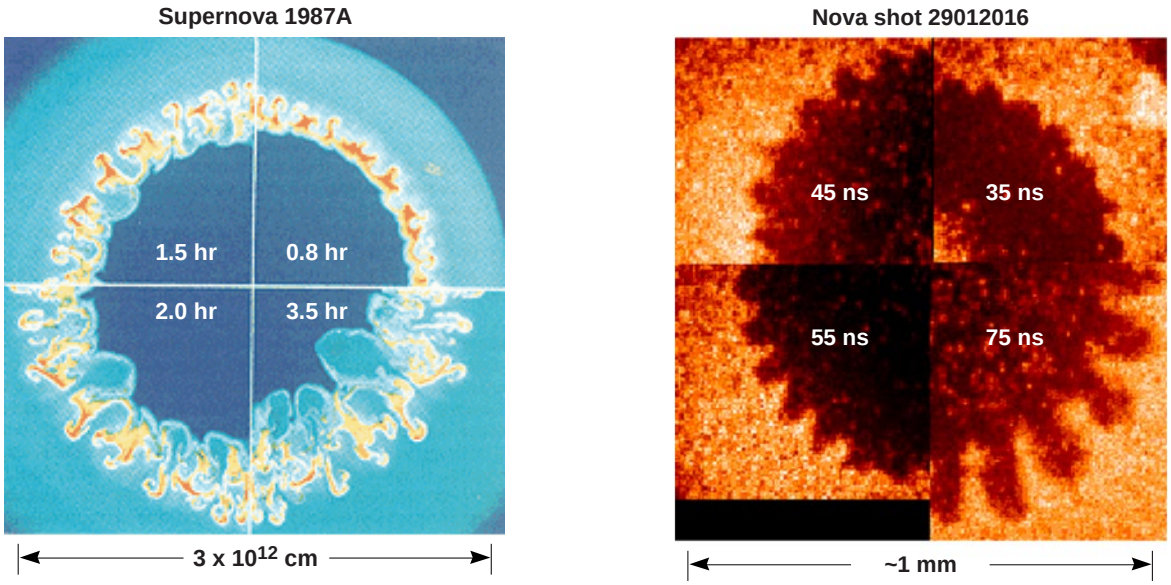

Figure 17. **Hydrodynamic instabilities occur in supernovae; scaled reproductions are created in laser experiments.[17, 18]**

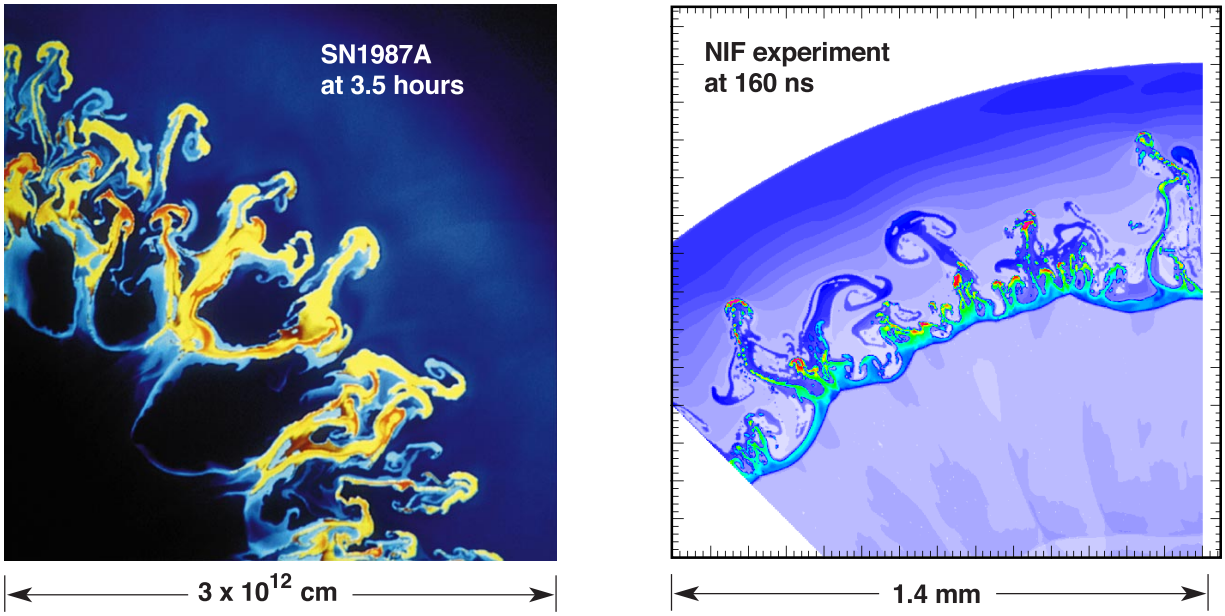

Figure 18. **More star-like, scaled supernova experiments are being designed for the NIF. These will be in spherically divergent geometry with multiple layers and multimode perturbations.[19, 20]**

Radiative Jets

Recent experiments have now begun to explore astrophysical phenomena where Euler's equation is no longer valid, i.e., when radiative transport is not negligible. Herbig-Haro or radiative jets are examples of such phenomena (Figure 19). Calculations indicate that such high Mach number jets undergo radial collapse to reestablish pressure equilibrium following radiative loss. Adiabatic jets, in contrast, remain extended in radius. Experiments at Nova and the Gekko laser at Osaka University have produced and diagnosed radiative jets using

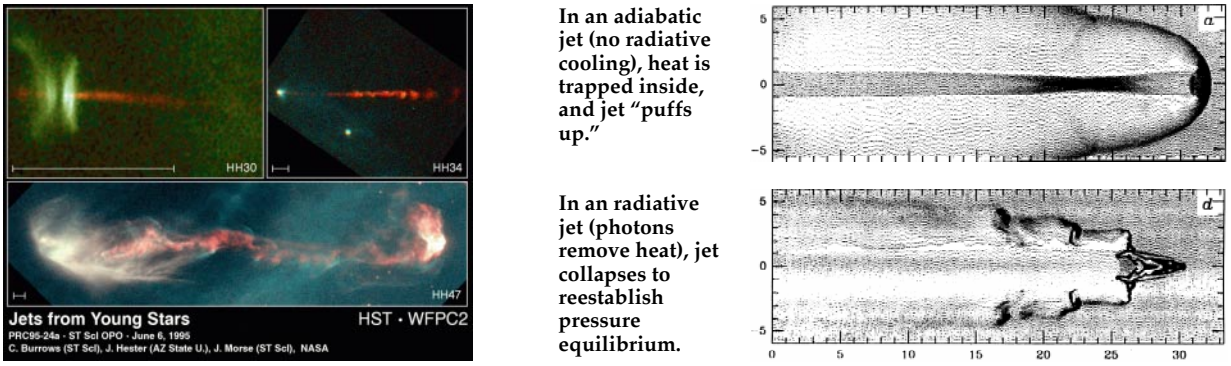

Figure 19. High Mach number jets occur in astrophysics and can be created in the laboratory using intense lasers.[21, 22]

innovative conical targets. Figure 20 shows calculated x-ray emission and absorption profiles of such a laboratory jet and comparison with experiments. This is excellent agreement including the jet's electron temperature of 250 eV (an adiabatic jet would have a temperature of 500 eV).

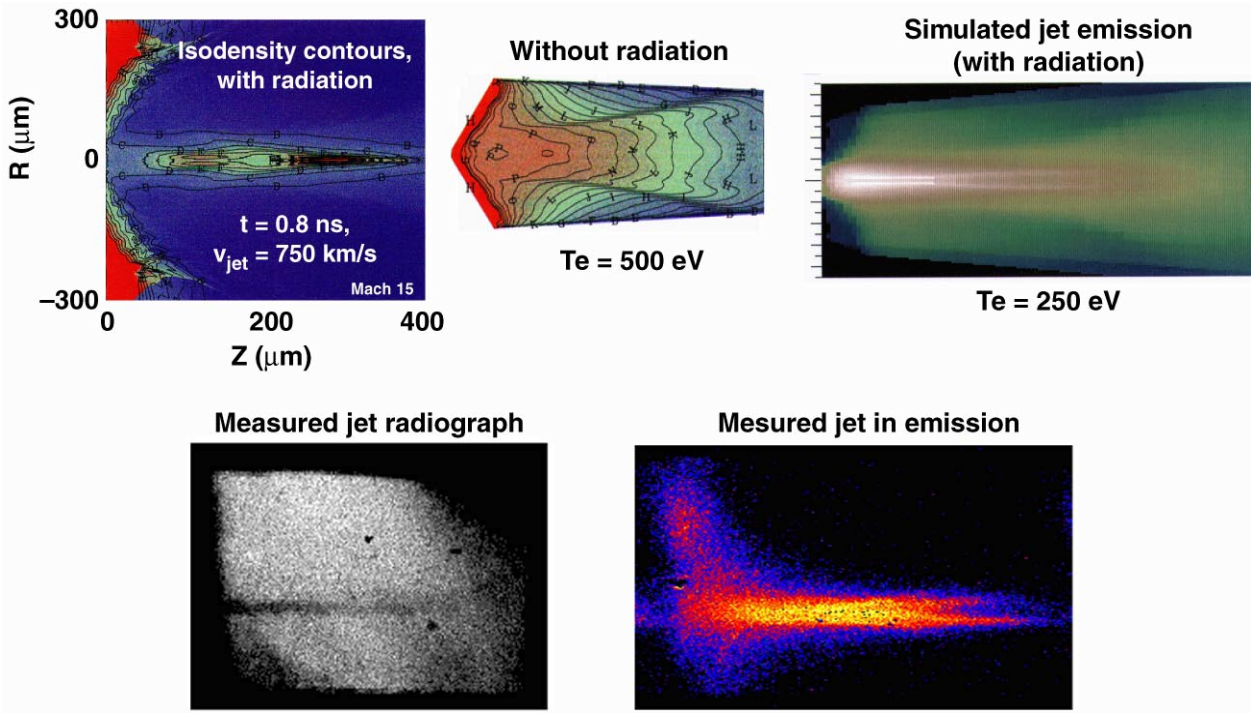

Figure 20. Simulations, experiment in remarkable qualitative agreement.[23]

Equation of State

An understanding of the equation of state (EOS) of hydrogen at pressures exceeding 1 Mbar is important for planetary science, brown dwarfs, and ICF. Study of the EOS along a principal Hugoniot for numerous materials up to tens of megabars has been made possible by ICF facilities. For example, a recent study of the compression of liquid deuterium at pressures from 0.2 Mbar to 3.4 Mbar using Nova has revealed high compressibility. This is now understood as linked to pressure-induced molecular disassociation corresponding to the transfer to "metallic

like" hydrogen. The results, shown in Figure 21, were obtained with numerous diagnostics. Similar insulator to metal transients have also been seen for LiF at ~6 Mbar and carbon (diamond) at ~10 Mbar.

Further experiments will study off-Hugoniot states of higher density and lower temperature using diamond anvils and temporally shaped laser pulses. If conditions of 100 g/cc and temperatures <1 eV can be reproduced, then pyconuclear fusion may result. Pyconuclear fusion occurs when the proximity of nuclei in cold compressed D-T tunnels through the Coulomb barrier producing significant fusion rates. The ability to conduct off-Hugoniot EOS measurements in materials such as H, He, H 2 O, N 3 , Si, and C at pressures exceeding tens of megabars with NIF will be of significant interest to a broad community.

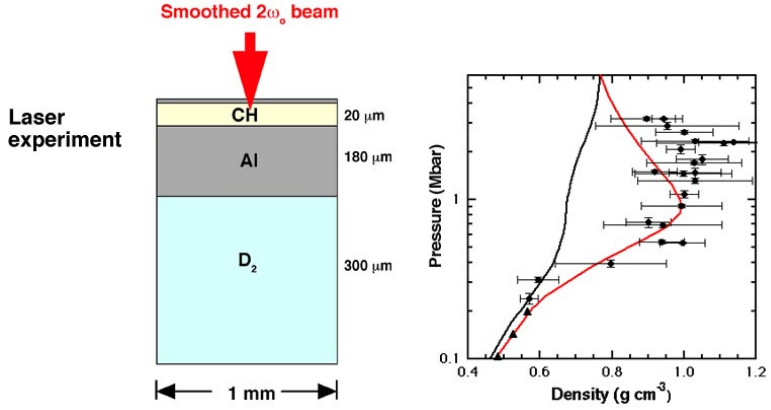

Figure 21. Laboratory experiments used Nova laser energy to produce a shock that allowed measurement of the equation of state of hydrogen at megabar pressures. This discriminated between competing models.[24]

V. Ultra High Energy Density Physics with Petawatt Lasers

The development of chirped pulse amplification has made possible extremely high-power (>10^{15} W), short-pulse (<10–12 sec), high-brightness lasers which can irradiate targets at intensities approaching 10^{21} W/cm^2.[25] Such lasers open up new opportunities in relativistic plasma physics. Experiments have shown that a significant fraction of high-intensity light is converted into relativistic electrons [26,27] with energies up to 100 MeV [27,28] as shown in Figure 22. Intense gamma rays created in electron collisions have led to the production of positrons,[28] also shown in Figure 22. As shown in Figure 23, these gamma rays induce (g,n) and (g,p) nuclear reactions,

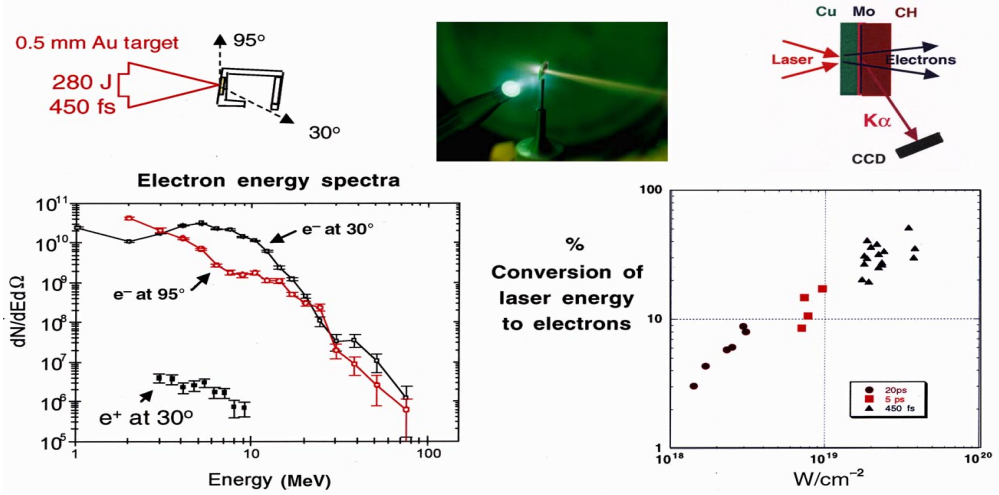

Figure 22. Petawatt experiments at >10^{20} W/cm^{-2} have produced relativistic electrons and initial evidence of electron–positron plasmas.

photo-dissociation of nuclei and activated radionuclides in a wide range of materials.[28,29] High-energy proton beams are generated and, in turn, induce strong (p,n) nuclear reactions. These data suggest that high-intensity lasers may provide new sources of ions, nuclear particles, and radionuclides which may have significant future scientific and technical applications.

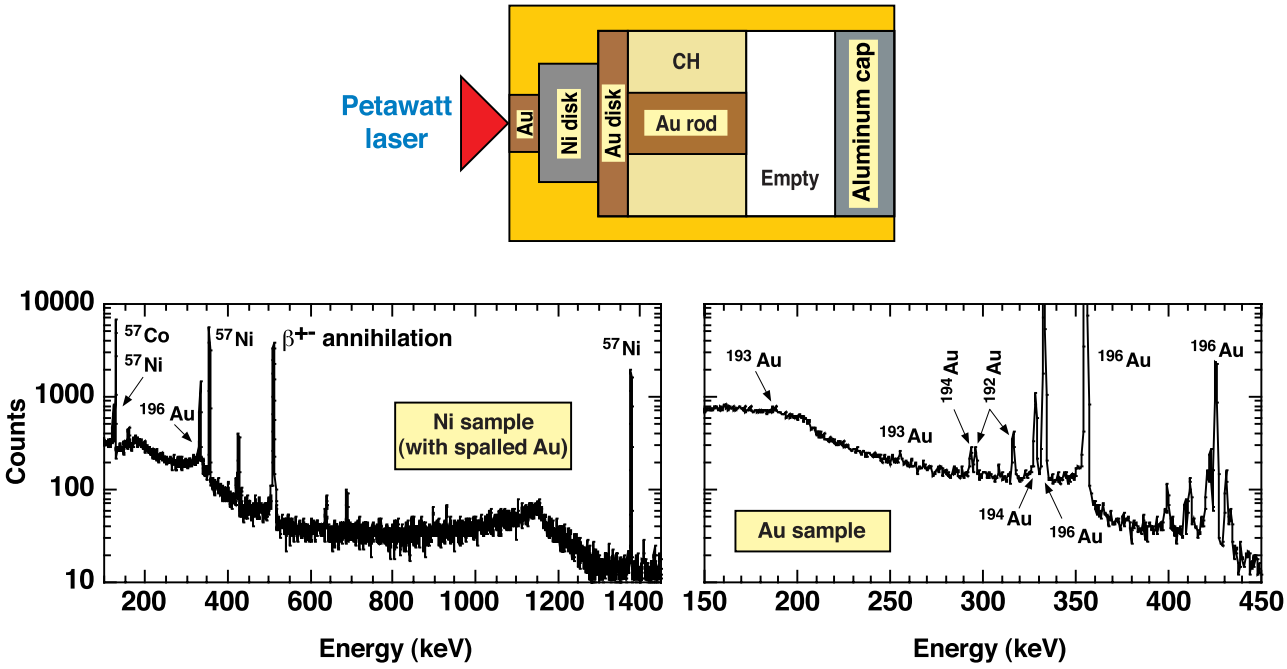

Figure 23. The Petawatt laser at LLNL has produced strong nuclear (g,xn) activation at thresholds exceeding 50 MeV .

VI. Conclusions

Inertial confinement fusion is poised to take its place in the community of fusion energy approaches. Significant challenges remain but the attractive energy features, affordable development plan, and construction of NIF provide a significant opportunity for development in the next decade. Finally, the richness of the science of ICF will help broaden the constituency for fusion and contribute to diverse fields as astrophysics and shock and condensed matter physics.

This work was performed under the auspices of the U.S. Department of Energy by Lawrence Livermore National Laboratory under contract No. W-7405-Eng-48.

References

1. L. Suter et al., "Status of Our Understanding and Modeling of Ignition Hohlraum X-Ray Coupling Efficiency," *ICF Quarterly Report,* **8**(4), 171, Lawrence Livermore National Laboratory, Livermore, CA, UCRL-LR-105821-98-4 (1999).
2. C. Labaune et al., "Non-linear modification of laser-plasma interaction processes under laser beams irradiation," *Phys. Plasmas,* **6,** 2048 (1999).
3. *Energy from Inertial Fusion,* W. Hogan, Scientific Ed. (IAEA, Vienna, 1995), Chapter 1.
4. J. D. Lindl, *Inertial Fusion Energy* (Springer-Verlag, New York, 1998), Chapter 13
5. *ICF Quarterly Report* **7**(3), Lawrence Livermore National Laboratory, Livermore, CA, UCRL-LR-105821-97-3 (1997
6. L. Suter et al., to be submitted, *Phys. Plasmas* (1999).
7. "Direct Drive Laser Fusion: Status and Prospects," *Phys. Plasmas,* 51901 (1998).
8. "Ion Beam Fusion," *Philos. Trans. R. Soc. London,* to be published (1999).
9. M. Cable et al., "Indirect driven, high convergence inertial confinement fusion implosions," *Phys. Rev. Lett.* **73**, 2316 (1994);
   B. A. Hammel et al., "X-ray spectroscopic measurements of high densities and temperatures from indirectly driven inertial fusion capsules," *Phys. Rev. Lett.* **70**, 1263 (1993).
10. S. W. Haan et al., "Design and Modeling of Ignition Targets for the National Ignition Facility," *Phys. Plasmas,* **2**(6), 2480 (June 1995).
11. John D. Lindl, *Inertial Confinement Fusion: the Quest for Ignition and Energy Using Indirect Drive* (Springer-Verlag, New York, 1998), p. 44.
12. Sakagami and Nishihara, *Phys. Fluids* **B 2**, 2715 (1990).
13. Hachisu et al., *Ap. J.* **368**, L27 (1991).
14. J. Kane et al., *Phys. Plasmas* **6**, 2065 (1999).
15. Kane et al., *Ap. J.* **478**, L75 (1997).
16. Remington et al., *Phys. Plasmas* **4**, 1994 (1997).
17. Muller et al., *Astron. & Astrophys.* **251**, 505 (1991).
18. Budil et al., to be submitted, *Astrophys. J.* (1999).
19. Muller, Fryxell, and Arnett, *Astron. & Astrophys.* **251**, 505 (1991).
20. J. Kane et al., *Phys. Plasmas* **6**, 2065 (1999).
21. C. Burrows, J. Hester, and J. Morse, *Jets from Young Stars,* PRC95-24a, ST Scl OPO, NASA (June 6, 1995).
22. Blondin et al., *Ap. J.* **360**, 370 (1990).
23. D. R. Farley et al., *Phys. Rev. Lett.,* in press (1999).
24. G. Collins et al., *Science* **281**, 1178 (1998).
25. M. D. Perry et al., *Opt Lett.* **24**, 160 (1999).
26. K. B. Wharton et al., *Phys. Rev. Lett.* **81**, 822 (1998).
27. M. H. Key et al., *Phys. Plasmas* **5**, 1966 (1998).
28. T. E. Cowan et al., *Lasers and Particle Beams* (in press).
29. T. E. Cowan et al., *Phys. Rev. Lett.* (submitted).